

CIC-7 requires Ostm1 as β -subunit to support bone resorption and lysosomal function

Supplementary Figures, Table and Methods

SUPPLEMENTARY FIGURES

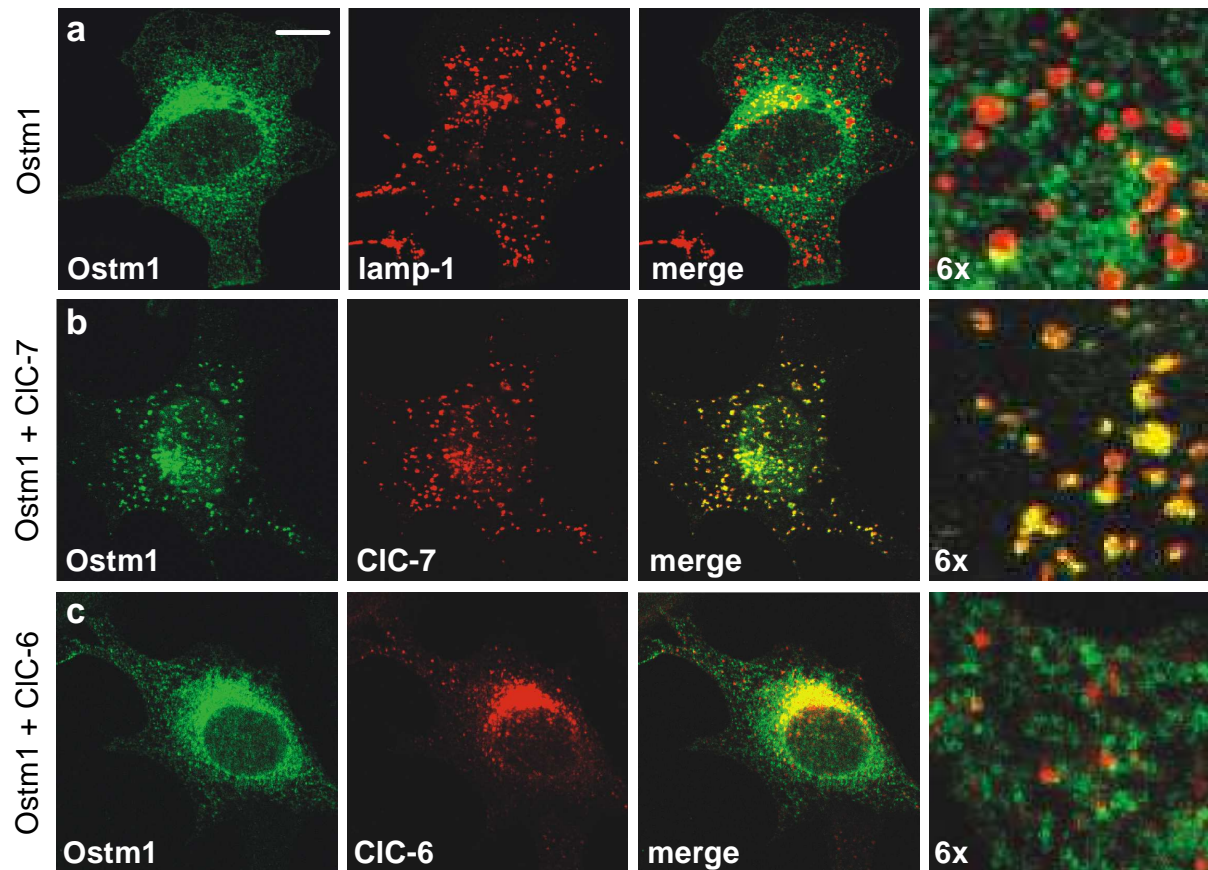


Figure S1. In contrast to CIC-7, CIC-6 has no effect on Ostm1 localization. **a**, Ostm1-transfected fibroblast showing a reticular and perinuclear Ostm1 staining that co-localised poorly with lamp-1. **b**, In fibroblasts co-transfected with Ostm1 and CIC-7, both proteins co-localised in vesicular structures. **c**, Co-transfecting Ostm1 with CIC-6 did not lead to a lysosomal localisation of Ostm1, nor to a significant co-localisation. *Clcn7*^{-/-} fibroblasts were used to avoid effects of endogenous CIC-7, but similar results were seen in HeLa cells. Scale bar indicates 10 μ m and 1.7 μ m for enlargements (right).

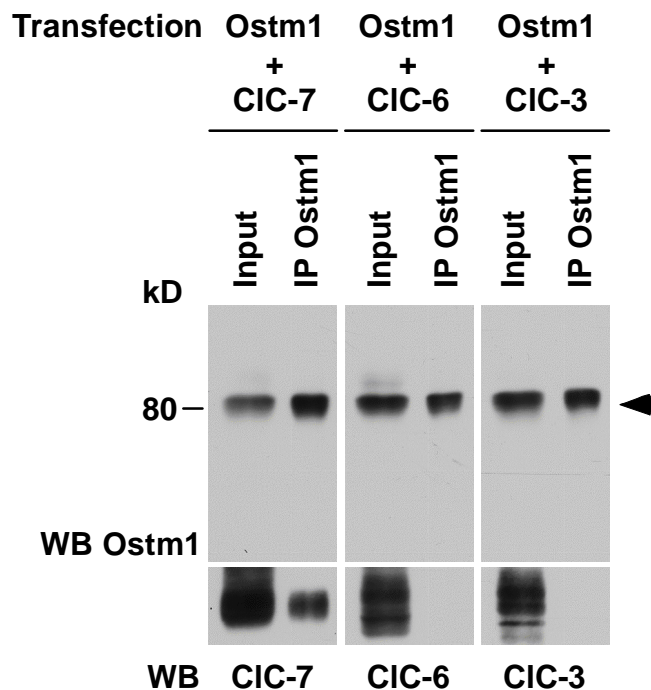


Figure S2. The ~80 kDa Ostm1 species interacts with CIC-7 in transfected HEK cells. Ostm1 was transiently co-expressed with the indicated CLC proteins in HEK293 cells. Upon such overexpression, only the ~80 kD (arrowhead), but not the 35-45 kD Ostm1 species was detected in Western blots. When Ostm1 was immunoprecipitated from transfected cell lysates using the guinea-pig antibody against the carboxyterminus of Ostm1, CIC-7 was co-precipitated. Thus, CIC-7 also interacts with the uncleaved Ostm1 species. By contrast, CIC-6 or CIC-3 could not be co-precipitated, demonstrating the specificity of the CIC-7/Ostm1 interaction.

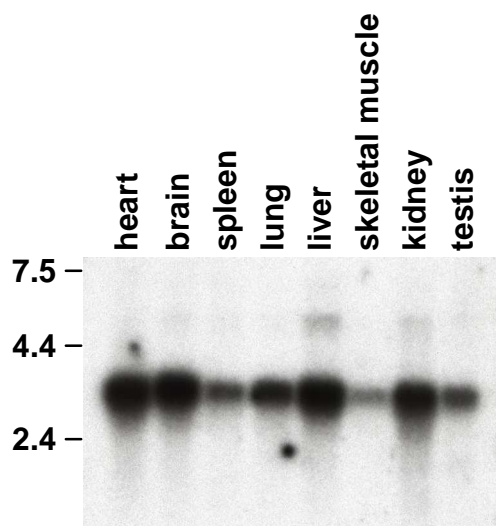


Figure S3. Ostm1 is ubiquitously expressed
Northern blot analysis on a mouse MTN™ Multiple Tissue Northern Blot (Clontech) using a ~1 kb Ostm1 cDNA probe reveals broad expression of Ostm1 (~ 3 kb).

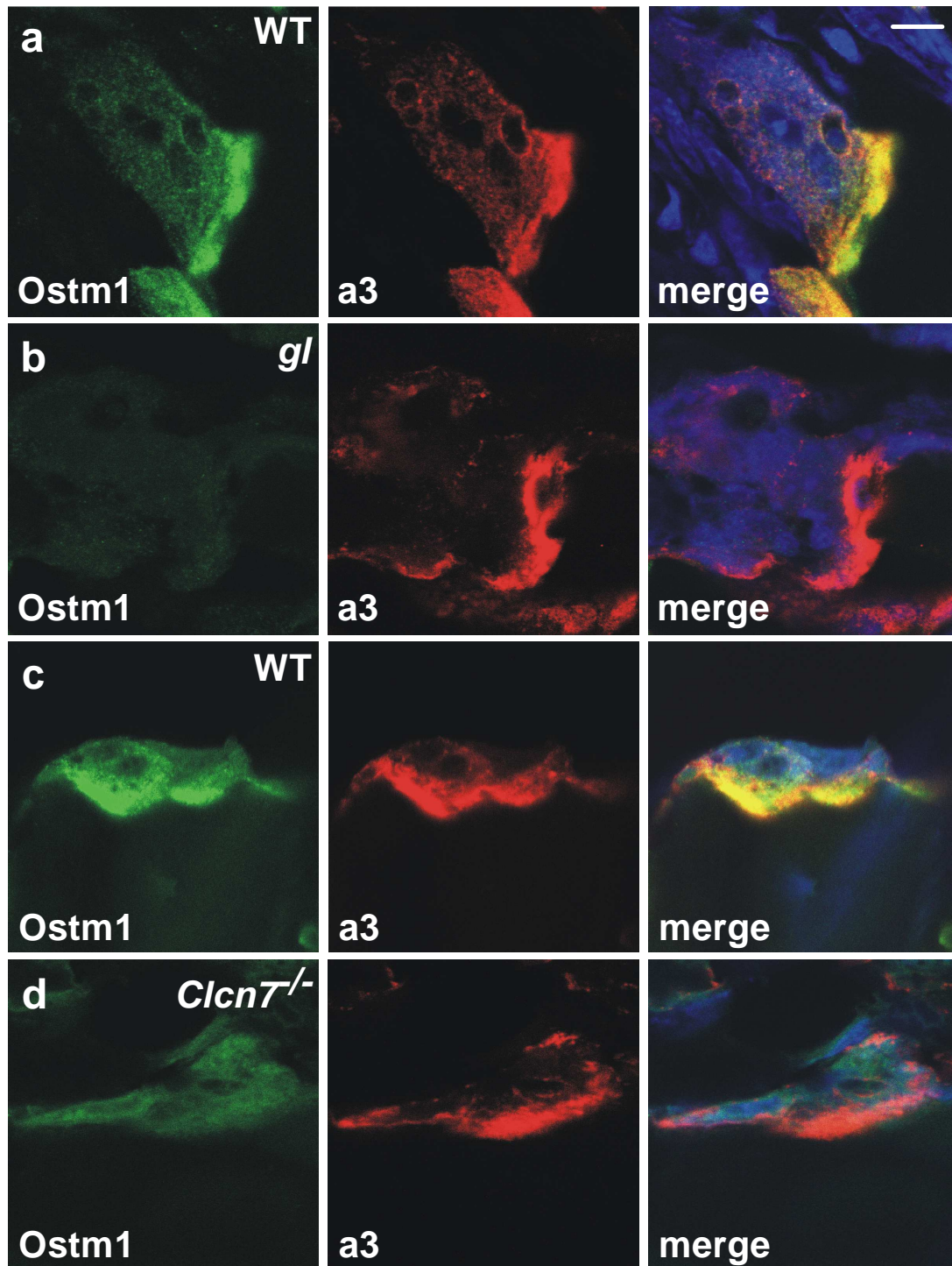


Figure S4. Ostm1 is undetectable in *Clcn7*^{-/-} osteoclasts. Paraffin sections of bone were co-stained for Ostm1 (green; rabbit antibody) and the a3 subunit of the V-type H⁺-ATPase (red; guinea-pig antibody). **a**, Ostm1 immunoreactivity co-localised with the a3 subunit in the ruffled border region of a bone-attached osteoclast and was absent in *gl* mice (**b**), demonstrating the specificity of the Ostm1 antibody. **c,d**, Ostm1 immunostaining (green) compared to a3 (red) in osteoclasts from WT (**c**) and CIC-7 KO (**d**) bone sections. In *Clcn7*^{-/-} bone, Ostm1 immunoreactivity was too low to be confidently distinguished from background fluorescence. No co-localisation was observed between the remaining Ostm1 signal and the a3 subunit. Counterstaining with TOTO-3 for nucleic acids is shown in blue in the merged images. Each WT/mutant pair was prepared, stained and scanned in parallel. Scale bar: 10 μ m for (a-b), 8 μ m for (c-d).

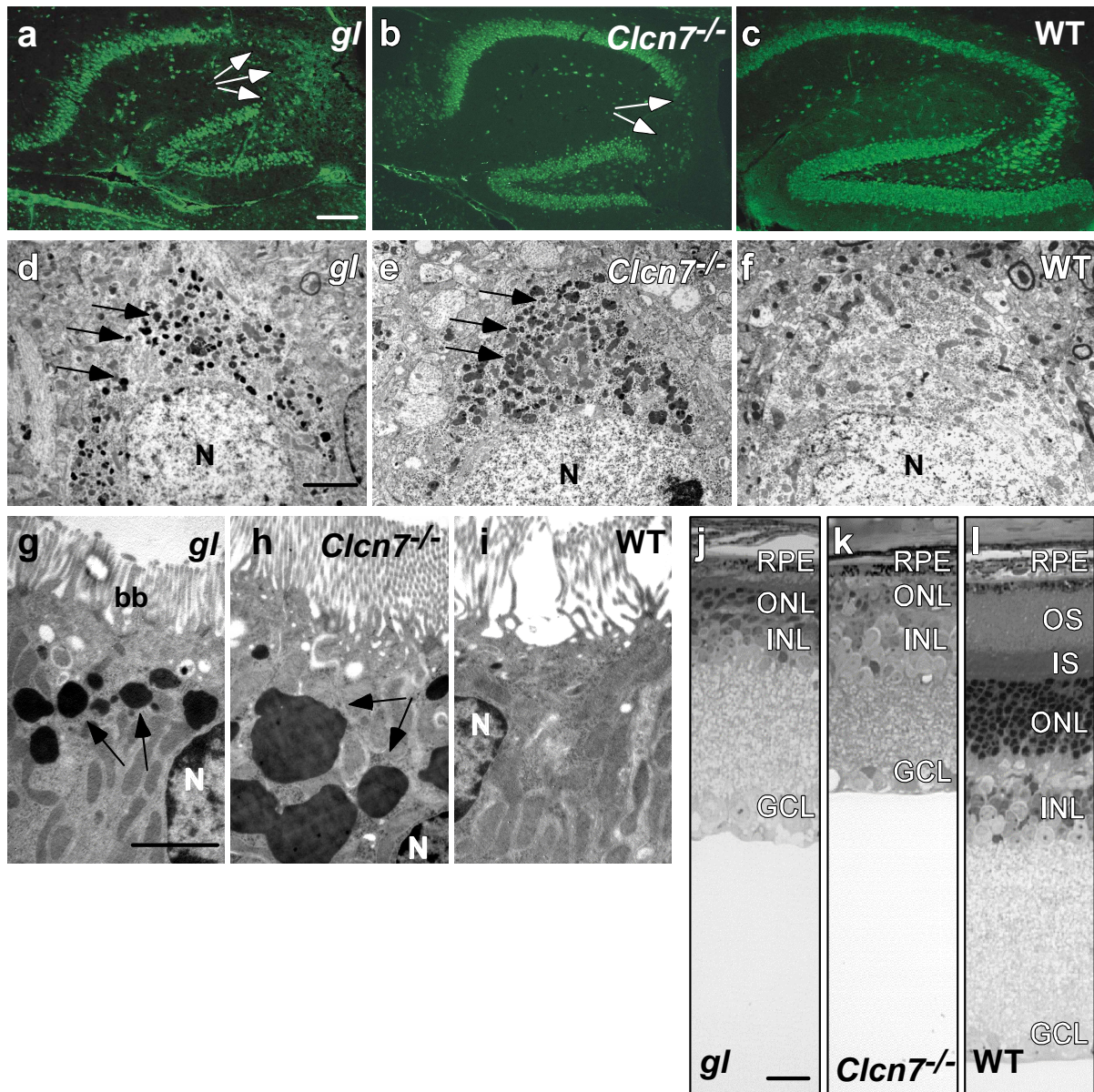


Figure S5. *Ostm1* deficiency leads to lysosomal storage and degeneration of the CNS and the retina, strikingly resembling the phenotype of *Clcn7^{-/-}* mice. Histological examination of *gl* mice revealed additional phenotypes in brain, retina and kidney. For better comparison, pictures demonstrating the corresponding, published phenotype of *Clcn7^{-/-}* mice^{1,2} are shown. **a-c**, Neurodegeneration in the hippocampus as revealed by NeuN staining. **(a)**, Neuronal cell loss (arrows) in the hippocampal CA3 region of a P47 *gl* brain. **(b)**, Similar region-specific cell loss was observed in a P30 *Clcn7^{-/-}* hippocampus, but not in WT controls at P47 **(c)**. **d-f**, Storage material in neuronal cell bodies. An electron micrograph of a cortical neuron from P44 *gl* brain **(d)** showed abundant electron-dense storage material (arrows) that resembled that found in P40 *Clcn7^{-/-}* neurons **(e)**. Such deposits were absent from P44 WT neurons **(f)**. **g-i**, Lysosomal storage in renal proximal tubules revealed by electron microscopy. **(g)**, Large electron-dense deposits (arrows) below the brush border (bb) of a proximal tubular cell of a P41 *gl* mouse, resembling those found in a P30 proximal tubular cell from *Clcn7^{-/-}* kidney **(h)**. No such deposits were found in P41 WT controls **(i)**. N, nucleus. **j-l**, Degeneration of the retina as investigated by methylene blue staining of semi-thin sections. **(j)**, degeneration of a P31 *gl* retina resembles that of a P30 *Clcn7^{-/-}* retina **(k)**. The photoreceptor cell layer and the inner

nuclear layer are severely reduced. (I), WT control (P31). RPE, retinal pigment epithelium; OS, photoreceptor outer segments; IS, photoreceptor inner segments; ONL, outer nuclear layer; INL, inner nuclear layer; GCL, ganglion cell layer. Scale bars: 100 μm (a-c), 2 μm (d-i), 20 μm (j-l).

In all aspects analyzed, *gl* mice resembled CIC-7 KO animals. In our laboratory, both homozygous mutant mice survived to an age of approximately 30 to 48 days. In addition, the described coat colour phenotype of *gl* mice^{3,4} was shared by CIC-7 KO animals. In a genetic background with agouti hair colour, *Clcn7*^{-/-} mice were grey (data not shown).

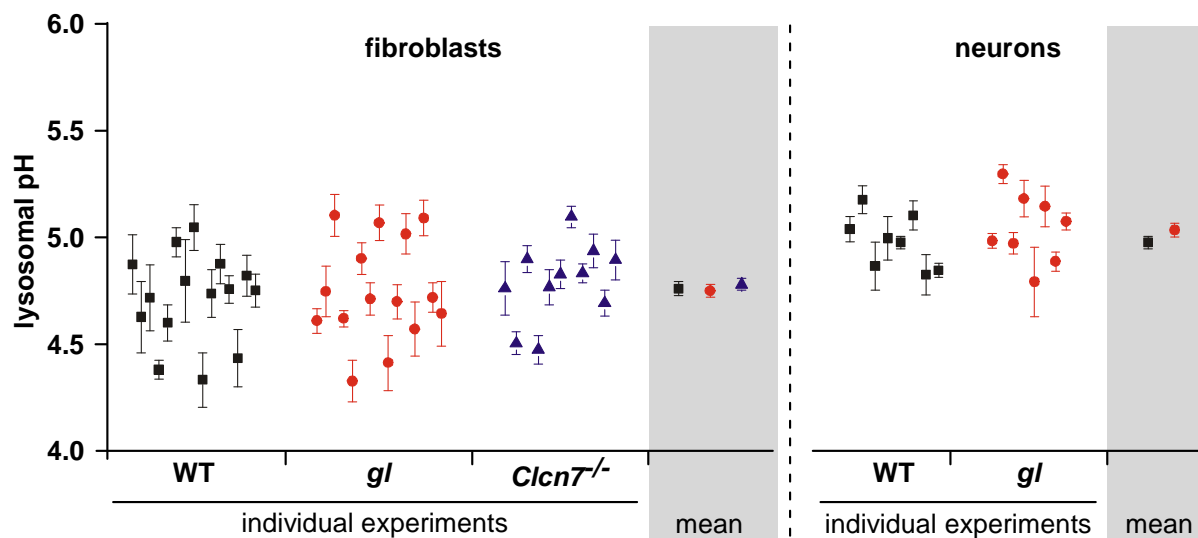


Figure S6. Lysosomal pH is not altered in *grey lethal* fibroblasts and cultured neurons.

Lysosomal pH of WT, *gl* and *Clcn7*^{-/-} fibroblasts or WT and *gl* neurons was determined by ratiometric imaging using a pH sensitive dye. Dextrane-coupled Oregon green 488 was loaded by endocytosis and chased into lysosomes. The average pH of lysosomes was 4.76 ± 0.03 (SEM) for WT, 4.75 ± 0.03 for *gl* and 4.78 ± 0.03 for *Clcn7*^{-/-} fibroblasts ($n = 109$ visual fields (containing one or two cells) for WT, 125 for *gl* and 108 for *Clcn7*^{-/-}). In cultured hippocampal neurons, the average pH of WT and *gl* lysosomes was 4.98 ± 0.03 and 5.04 ± 0.03 , respectively ($n = 69$ for WT and 76 for *gl*). In our previous work², we had found no difference in lysosomal pH between WT and *Clcn7*^{-/-} mice, either.

SUPPLEMENTARY TABLE

CIC-7 mRNA levels in *gl* mice are unchanged, and *vice versa*.

	CIC-7 mRNA level (<i>gl</i> /WT)	Ostm1 mRNA level (<i>Clcn7</i> ⁻ /WT)
Brain	1.10 ± 0.03 (n=4)	1.35 ± 0.04 (n=4)
Kidney	0.97 ± 0.10 (n=4)	1.11 ± 0.08 (n=3)
Liver	0.85 ± 0.03 (n=4)	1.07 ± 0.03 (n=4)
Bone	1.09 ± 0.10 (n=4)	1.23 ± 0.37 (n=6)

RNA from *gl* / WT and *Clcn7*⁻ / WT littermate pairs was isolated from the indicated tissues and transcribed into cDNA. CIC-7 and Ostm1 transcript levels were examined by real-time PCR. Shown is the fold change (± SEM) comparing mutant mice to the respective WT animals (n: number of animals analyzed). No significant alterations were observed, demonstrating that the loss of CIC-7 in *gl* mice and the absence of the 35-45 kD Ostm1 species in *Clcn7*⁻ mice are not due to changes at the transcriptional level.

SUPPLEMENTARY METHODS

Antibodies. Rabbit antibodies against CIC-7 were published¹. A corresponding guinea pig antiserum was raised against the same amino-terminal peptide (GRDRDDEEGAPLL-C). Antibodies against the $\alpha 3$ subunit of the V-type H⁺-ATPase were raised in rabbits and guinea pigs (peptide PDASTLENSWSPDEEK-C). Peptides were coupled to keyhole limpet hemocyanin (KLH) via the C-terminal cysteine residues. Their specificity was proven by control stainings on tissues from *Clcn7*⁻ or *oc/oc* mice^{2,5}, respectively. Ostm1 antibodies were raised in guinea pigs and rabbits against the peptide C-LKSSTSFANIQENAT, which was coupled to albumin via the N-terminal cysteine. The guinea pig antibody was used for immunoprecipitation, while all other experiments were performed with the rabbit antiserum. The CIC-3 antibody was published⁶, and the CIC-6 antibody will be described in detail elsewhere. All above-mentioned antibodies were purified by affinity to the corresponding peptides. Commercial antibodies were: rat anti-lamp-1 and -2 (clones 1D4B and ABL-93, BD Pharmingen), rabbit anti-actin (Sigma), mouse anti-PDI (StressGen), rabbit anti-calnexin (Biomol), mouse anti-NeuN (Chemicon), rabbit anti-rab4 (Santa Cruz) and rat anti-HA (3F10, Roche). Secondary antibodies were labelled with Alexa 488 and 546 dyes (Molecular Probes) or HRP (Jackson ImmunoResearch). TOTO-3 was from Molecular Probes. The cathepsin D antibody was a gift from R. Pohlmann (Münster).

DNA constructs. Mouse *Ostm1* was cloned from kidney cDNA and subcloned into pEGFP-N3 (Clontech) from which the sequence encoding GFP was removed and replaced by an in-frame stop codon, or an *HA* epitope (YPYDVPDYA) followed by a stop codon, resulting in the C-terminal sequence ENAT-VD-*HA*. To tag the putative signal peptide, an *HA* epitope was inserted after the first methionine (resulting sequence: M-*HA*-RDAEL). A mutant mimicking the *Ostm1* fragment remaining in a human osteopetrosis patient³ was generated by replacing sequence encoding amino acids 266-338 by an *HA*-epitope (resulting sequence: VEDA-VD-*HA*). Rat CIC-7 and human CIC-6 cDNAs⁷ were subcloned into pFrog and pcDNA3.1, respectively. Detailed cloning and sequence information is available from the authors upon request.

Cell culture and immunostaining. HeLa cells, WT and CIC-7 knockout fibroblasts were cultured as described², seeded onto glass coverslips and transfected with FuGene (Roche) according to the information of the supplier. Per coverslip, 500 ng plasmid encoding CLC proteins and 10 ng plasmid encoding *Ostm1* constructs were used (to achieve moderate expression levels). In all transfections, the total DNA amount was kept constant with empty expression vector. After 24 to 36 hours of expression, immunostaining was done as described². For protease inhibitor treatment, WT fibroblasts were incubated with 20 μ M leupeptin (Roche) or 10 μ M E64 for 24 hours. Cells were harvested in HEPES-buffered saline (HBS), pH 7.4, pelleted at 1000xg and lysed in HBS containing 1% (v/v) Triton X-100. The supernatant of a 20,000xg spin was used for SDS-PAGE and Western blot analysis.

Biochemical methods. Cellular membranes were fractionated by sedimentation velocity centrifugation in a Percoll gradient. Per gradient, 80 mg of mouse brain were homogenized with a potter in 250 mM sucrose, 3 mM imidazole pH 7.4. A postnuclear supernatant was prepared by 1000xg centrifugation and loaded on top of a 36 ml Percoll gradient (Pharmacia, 17% in homogenization buffer). After centrifugation at 38,760xg for 35 min, 3 ml fractions were collected and re-centrifuged at 125,000xg. The opaque band was withdrawn with a pipette in 400 μ l volume, adjusted to 1% (v/v) Triton X-100 and centrifuged again at 125,000xg. The supernatant of the Percoll pellet was used for protein determination (BCA, Pierce), in deglycosylation experiments and denatured for SDS-PAGE and Western blot.

For deglycosylation, 160 μ g of a brain membrane preparation (140,000xg pellet) or 30 μ g of fraction 1 (lysosomes) or 80 μ g of fraction 11 (light membranes) from a Percoll gradient were used. Samples were denatured at 55°C for 5 minutes in 100 mM NaH₂PO₄, 0.2% (w/v) SDS and 0.1% (v/v) β -mercaptoethanol for PNGaseF (Roche) or 50 mM NaAcetate pH 5.2, 0.02% SDS, 0.1% β -mercaptoethanol for Endo H (Roche) treatment. After adjusting to 1% (v/v) Triton X-100 and 1.3 mM EDTA, complete protease inhibitor (Roche) and 1 unit of PNGase F or 0.025 units of EndoH were added and samples incubated at 37°C for 30 min .

For preparation of protein lysates, the bones of mouse hindlimbs were ground in liquid nitrogen. The powder was dissolved in HEPES-buffered saline (HBS), pH 7.4 containing 1% (v/v) Triton X-100 and 0.1% (w/v) SDS. Debris was pelleted at 20,000xg and the supernatant separated by SDS-PAGE.

For immunoprecipitation of endogenous proteins, brain homogenates were prepared in MES buffered saline (MBS) pH 6.5 with a douncer. The supernatant of a 1000xg spin was again centrifuged at 100,000xg for 50 min to pellet membranes, which were dissolved in lysis buffer (MBS pH 6.5, 1% Triton X-100, 2.5 mM CaCl₂, 2.5 mM MgCl₂). Samples were again centrifuged at 70,000xg to pellet non-solubilized material and supernatants were used for immunoprecipitation.

For immunoprecipitation of overexpressed proteins, HEK293 cells were transfected using calcium phosphate precipitation⁸. After 24 to 48 hours, cells were harvested in HBS, pH 7.4, pelleted at 1000xg and lysed in HBS containing 1% (v/v) Triton X-100, 2.5 mM each of CaCl₂ and MgCl₂ and complete (Roche) protease inhibitors. The supernatant of a 20,000xg spin was used for co-immunoprecipitation.

Antibodies were incubated with protein A sepharose in PBS for one hour at room temperature on an overhead rotator. They were washed twice with 0.2 M Na-borate pH 9.0 followed by crosslinking the antibodies to the protein A sepharose with 5.2 mg/ml dimethylpimelidate (Pierce) in borate buffer for 30 minutes. The reaction was stopped by washing with TBS pH 7.4 and excess antibody was removed by washing with 0.2 M glycine/Cl pH 2.5. Protein samples were incubated with crosslinked antibodies for 2 hours at 4°C and unbound material was removed by washing 4x with 1 ml lysis buffer. Bound proteins were eluted with 100 µl 0.1 M glycine/Cl pH 2.8, neutralized and denatured using SDS sample buffer.

Secretion of the Ostm1 truncation mutant Δ(266-338) was analyzed in HEK293 cells. 24 hours after transfection with Ostm1-HA or Ostm1Δ(266-338)-HA cDNAs, cells were cultured in serum-free DMEM medium. 12 hours later, the supernatant was collected and centrifuged twice at 2650xg to remove dead cells and debris. The cells were harvested in 250 mM sucrose, 25 mM HEPES, pH 7.4, homogenized in a douncer and centrifuged at 1000x g to obtain a postnuclear supernatant (S1). Aliquots of S1 (3%) and culture supernatant (0.25%) were analyzed by Western blotting for the HA epitope.

Proteins were separated by SDS-PAGE and blotted onto Optitran nitrocellulose membranes (Schleicher&Schuell). After blocking in 3% non-fat dry milk with 0.2% (v/v) NP-40 in PBS, antibody incubation was done overnight in blocking buffer at 4°C. Membranes were washed 4 times with P BS, incubated with secondary antibody for 2 h and washed again. Detection used chemoluminescence (SuperSignal West pico or femto, Pierce) and Kodak X-Omat Blue XB-1 film or the ChemiDoc (BioRAD) CCD camera system. Densitometric analysis was performed on films scanned with an Epson Expression 1680 Pro scanner or images obtained by the CCD camera using Tina 2.0 (Raytest) or Quantity One (BioRAD) software, respectively. For quantification of Western blots (Fig. 4g), serial dilutions of the lysates were compared to avoid any non-linearity of the detection method.

The apparent weight of Ostm1 differed depending on the SDS-PAGE gel system used. Large and small forms ran at 80 kD/35-45 kD in Bis-Tris gradient gels (Invitrogen) with MES running buffer, 70/35-40 kD in the same gel system with MOPS running buffer and 50 kD/30-35 kD in standard 10 or 11.5% Tris/Cl gels with Tris/glycine buffer⁹ when compared to Benchmark prestained molecular weight markers (Invitrogen). For simplicity, the molecular weight of Ostm1 species is uniformly indicated as 80 kD/40 kD in the figures. In figures 1 and 3, some blots for Ostm1 were slightly compressed in height to display bands at comparable positions.

Immunohistochemistry and histology. Procedures for immunostainings on cryo- and paraffin sections and histology were described². Bone sections were treated with rapid decalcifier (Eurobio, Les Ulis, France) before paraffin embedding.

Real-Time PCR. Clcn7 and Ostm1 RNA levels were determined by real-time PCR as described².

Northern Blot Analysis. Mouse MTNTM Multiple Tissue Northern Blot was purchased from Clontech, BD Bioscience. RNA was hybridized to random-primed, ³²P labeled, mouse-specific 1030 bp Ostm1 probe (activity 2x10⁶ cmp/ml

ExpressHyb solution) according to the Clontech protocol. The blot was exposed for autoradiography for 48 h at -70°C on Kodak BioMax M R film.

Lysosomal pH measurement. Primary cultures of hippocampal neurons were prepared from newborn *gl* and WT littermate mice and loaded with indicator dye as described before². Immortalized and non-immortalized primary WT, *gl* and CIC-7 knockout mouse fibroblasts were loaded for two hours with 0.3 mg/ml dextran-coupled Oregon Green 488 (Molecular Probes) in DMEM with 10% fetal calf serum and chased for two hours in the culture medium. Ratiometric fluorescence microscopy, image acquisition and analysis were performed as described previously². During pH measurements, cells were incubated in bicarbonate buffered Ringers buffer (in mM 115 NaCl, 25 NaHCO₃, 3 KCl, 2 KH₂PO₄, 1 CaCl₂, 1 MgSO₄, 5 HEPES, 10 Glucose, pH 7.4) gassed with 5% CO₂ in air. Calibration curves were obtained by subsequent treatment with MES or HEPES buffers (in mM 5 NaCl, 1 CaCl₂, 115 KCl, 1.2 MgSO₄, 25 MES or HEPES) containing monensin and nigericin (1mM each). Solutions ranging from pH 6.5 to 4.0 were applied for 5 min each.

REFERENCES

1. Kornak, U. et al. Loss of the CIC-7 chloride channel leads to osteopetrosis in mice and man. *Cell* **104**, 205-215 (2001).
2. Kasper, D. et al. Loss of the chloride channel CIC-7 leads to lysosomal storage disease and neurodegeneration. *EMBO J* **24**, 1079-1091 (2005).
3. Chalhoub, N. et al. Grey-lethal mutation induces severe malignant autosomal recessive osteopetrosis in mouse and human. *Nat Med* **9**, 399-406 (2003).
4. Boyce, B. F. Bad bones, grey hair, one mutation. *Nat Med* **9**, 395-396 (2003).
5. Scimeca, J. C. et al. The gene encoding the mouse homologue of the human osteoclast-specific 116-kDa V-ATPase subunit bears a deletion in osteosclerotic (*oc/oc*) mutants. *Bone* **26**, 207-213 (2000).
6. Stobrawa, S. M. et al. Disruption of CIC-3, a chloride channel expressed on synaptic vesicles, leads to a loss of the hippocampus. *Neuron* **29**, 185-196 (2001).
7. Brandt, S. & Jentsch, T. J. CIC-6 and CIC-7 are two novel broadly expressed members of the CLC chloride channel family. *FEBS Lett* **377**, 15-20 (1995).
8. Chen, C. & Okayama, H. High-efficiency transformation of mammalian cells by plasmid DNA. *Mol Cell Biol* **7**, 2745-52 (1987).
9. Laemmli, U. K. Cleavage of structural proteins during the assembly of the head of bacteriophage T4. *Nature* **227**, 680-5 (1970).